

Nanostructural and local electronic properties of Fe/W(110) correlated by scanning tunneling spectroscopy

M. Bode, R. Pascal, M. Dreyer, and R. Wiesendanger

Institute of Applied Physics and Microstructure Research Center, University of Hamburg,

Jungiusstrasse 11, D-20355 Hamburg, Germany

(Received 24 May 1996)

Epitaxial Fe(110) films grown on W(110) substrates exhibit, up to the second pseudomorphic monolayer, a peak in dI/dU spectra at 0.2 eV above the Fermi level as measured by scanning tunneling spectroscopy (STS). It is shown directly by STS on nanometer-scale wedges of Fe/W(110) that the density of empty states is diminished wherever the stressed Fe film begins to relax. The change in local differential conductivity can therefore be explained by a stress-induced change of electronic structure for the first two monolayers due to the large misfit between film and substrate. [S0163-1829(96)52136-3]

Research on thin solid films is of great interest since they offer the opportunity to study both reduced symmetry and interface effects. Furthermore, it is possible by heteroepitaxial, pseudomorphic growth to stabilize solids in structures, i.e., with crystalline symmetries and lattice constants, that are far from those of the corresponding bulk material. This facilitates creating materials with properties that do not exist in nature. Strong effort has been made to investigate electronic and magnetic properties of thin ferromagnetic $3d$ transition-metal films on both noble metal substrates, such as Fe/Cu(100),¹ and Co/Cu(100),² as well as refractory $5d$ transition-metal substrates with high melting temperatures, such as Fe/W(110).³⁻¹² Particularly, Fe shows an interesting growth behavior on W(110) which has been studied in great detail by other authors.^{10,12,13} Both Fe and W have a bcc crystal structure. Although there is a large lattice misfit of 9.4% it is known that Fe grows pseudomorphically on W(110) in the first monolayer (ML). At room temperature the growth is dominated by two-dimensional islands which do not coalesce up to a coverage of 0.6 ML. At a substrate temperature of 570 K the growth mode changes to step flow and at a coverage $\Theta = 1.3$ ML the Fe film begins to relax. The onset of relaxation in the second Fe layer is indicated by dislocation lines along the $[001]$ direction with an average separation of 46 Å. The dislocation lines become periodic (separation of 27 Å) when the local coverage is 3 ML. From the fourth layer on the Fe film exhibits a two-dimensional periodic dislocation network. This is caused by a moiré pattern due to the insertion of extra iron rows in order to compensate for the misfit between Fe(110) and W(110). Some atoms are then forced to occupy nonlattice sites. These results could be confirmed during our experiments. It should be added that the growth of Fe/W(110) is closely related to the magnetic properties as reported earlier by other authors.^{8,11}

In this paper we report on a STS study of Fe grown on W(110). To our knowledge, we observed for the first time directly in real space a stress-induced change of electronic structure of thin films by STS. For pseudomorphically grown Fe on W(110) this results in an increased density of states just above the Fermi level E_F . On atomically flat nanometer-

scale wedges of Fe/W(110) we show that the empty-state density close to E_F is diminished wherever the Fe film begins to relax. Spectroscopic data measured close to island edges of a submonolayer Fe film show that the island edges are partially relaxed due to the reduced number of next nearest neighbors, which hinders coalescence as proposed earlier by Elmers *et al.*⁸

The Fe films were prepared in ultrahigh vacuum (UHV, base pressure $p < 5 \times 10^{-11}$ torr) on W(110) substrates held at room temperature by using an electron-beam evaporator with integrated flux control. During evaporation the pressure did not exceed 4×10^{-10} torr. The cleanliness of the sample surface was checked by means of low-energy electron diffraction (LEED) and Auger electron spectroscopy (AES). Upon thin-film growth the sample was transferred *in situ* into our UHV scanning tunneling microscope (STM). All topographic data were obtained in the constant current mode with electrochemically etched tungsten tips. The spectroscopic data were measured by adding an ac component to the gap voltage ($U_{\text{mod}} = 30$ mV; $\nu = 2.77$ kHz). We detected the differential conductivity dI/dU of the tunnel junction by the lock-in technique. Typical tunneling parameters were $I_{\text{tun}} = 1-3$ nA and $U_{\text{gap}} = \pm 1.0-1.5$ V.

Figure 1(a) shows the topography of a submonolayer Fe film ($\Theta \approx 0.45$ ML) grown at room temperature. The topography is dominated by 2D islands. A small amount of the deposited material tends to decorate the monoatomic steps of the substrate. A map of the differential conductivity dI/dU of the same sample at several gap voltages is shown in Fig. 1(b). During the scan the gap voltage was changed every 80 scan lines in steps of 0.2 eV. Obviously the contrast between islands and substrate flips. First, at $U_{\text{gap}} = 1.0$ V the W(110) substrate appears brighter than the Fe islands, i.e., W exhibits a higher differential conductivity than Fe [Fig. 1(b)]. This situation remains unchanged up to a gap voltage $U_{\text{gap}} = 0.6$ V. If the gap voltage is further diminished to $U_{\text{gap}} = 0.4$ V the contrast flips and the Fe islands appear brighter than the W substrate. This flip of contrast does not occur homogeneously on individual islands. In contrast, the data measured at $U_{\text{gap}} = 0.4$ V show clearly that on top of the Fe islands significant variations in the differential conductivity exist which

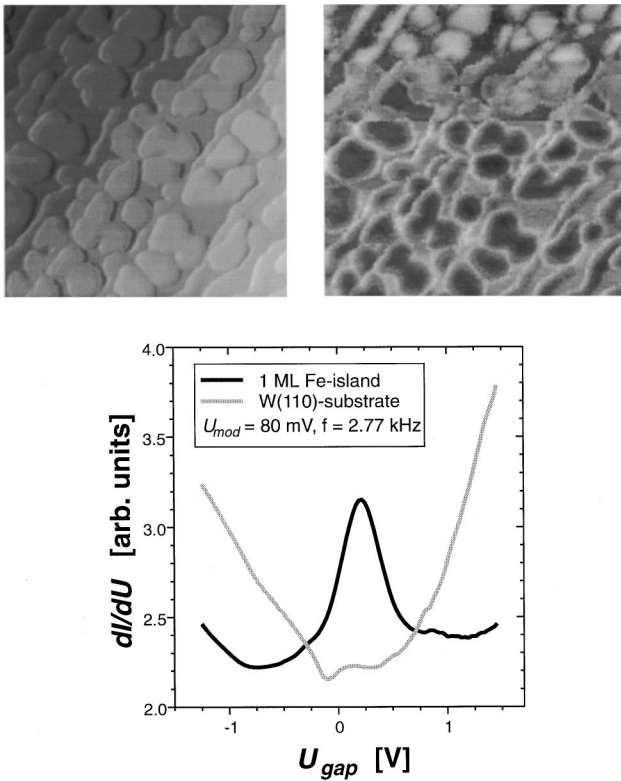


FIG. 1. (a): Topography of 0.45 ML Fe on W(110) (scan range: $250 \text{ nm} \times 250 \text{ nm}$). During evaporation the substrate was held at room temperature. The deposited material forms monolayer islands and a small amount decorates the step edges. Maps of the differential conductivity dI/dU are shown in (b). During the scan the gap voltage was decreased every 80 lines by 0.2 V. Bright and dark areas correspond to high and low differential conductivity, respectively. The contrast between Fe and W flips between $U_{gap} = 0.6$ V and $U_{gap} = 0.4$ V. While W has the higher differential conductivity in the range $0.6 \leq U_{gap} < 1.0$ V (lower part of the image), the opposite is true in the upper part. (c) Averaged spectra of the differential conductivity dI/dU taken above Fe and W sites from the former image. Obviously one monolayer of Fe on W(110) exhibits an empty-state peak which is centered at $U_{gap} = 0.22$ V while the spectrum of the bare W(110) substrate is relatively featureless in this bias regime.

will be discussed below. The contrast becomes maximal at $U_{gap} = 0.2$ V. This behavior can be understood based on local tunneling spectroscopy data [Fig. 1(c)]. The curves represent averages over 100 spectra measured above the Fe monolayer and the W substrate, respectively. While the plot of differential conductivity dI/dU versus gap voltage of the Fe monolayer exhibits a peak which is centered at $U_{gap} \approx 0.2$ V (empty sample states), W shows no significant features in the gap voltage range under study.

To check if the empty-state peak is characteristic for a thin film of Fe on W(110) or if it is also present on bulklike Fe(110), we prepared a sample which contains simultaneously different regimes of coverage, thin films of monolayer and bilayer thickness and 3D-like islands. We evaporated 3 ML of Fe on the W(110) substrate and postannealed the sample at a temperature $T > 600$ K for 2 min. This results in a topography as displayed in Fig. 2(a). The islands have a thickness between 4 ML and 8 ML while between them we

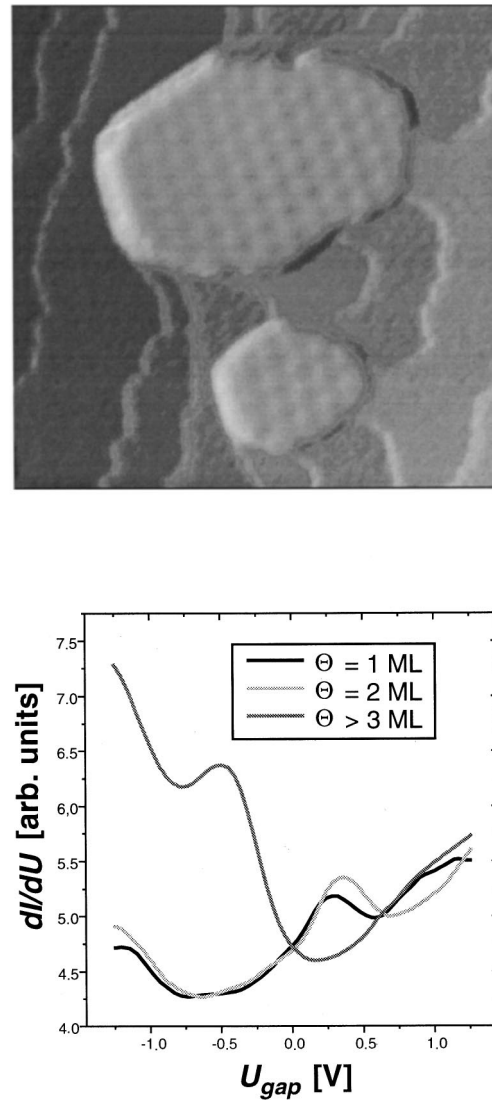


FIG. 2. (a): Constant current image (scan range: $50 \text{ nm} \times 50 \text{ nm}$) of a 3-ML Fe film on W(110). The film was postannealed at $T > 600$ K. After annealing the substrate is covered by islands with a local coverage of 4–8 ML. Since extra rows of Fe are inserted to compensate the stress in the film the surfaces of the islands exhibit a periodic two-dimensional dislocation network. Between the islands the coverage of the pseudomorphic Fe film is 1.3 ML. (b): Averaged spectra of the differential conductivity dI/dU taken above positions where the local coverage is 1 ML, 2 ML or more than 3 ML. While we find an empty-state peak on pseudomorphic films (i.e., in the first and second monolayer) this peak does not appear above the islands. Instead, we measure an occupied-state peak at $U_{gap} \approx -0.5$ eV above thick islands.

found one or two monolayers grown in the step flow mode. The STS data were averaged over 50 spectra from the three different regimes of coverage: 1 ML, 2 ML, and > 3 ML [Fig. 2(b)]. Surprisingly the empty-state peak is present above the first and second pseudomorphic monolayer but it does not appear in the dI/dU spectra, which were measured above the 3D islands. In contrast, above the islands we measured a peak at $U_{gap} = -0.5$ V (occupied states). A similar spectrum was also measured on islands with a height of 30–50 ML where we could no longer observe the two-dimensional periodic network. This occupied-state peak cor-

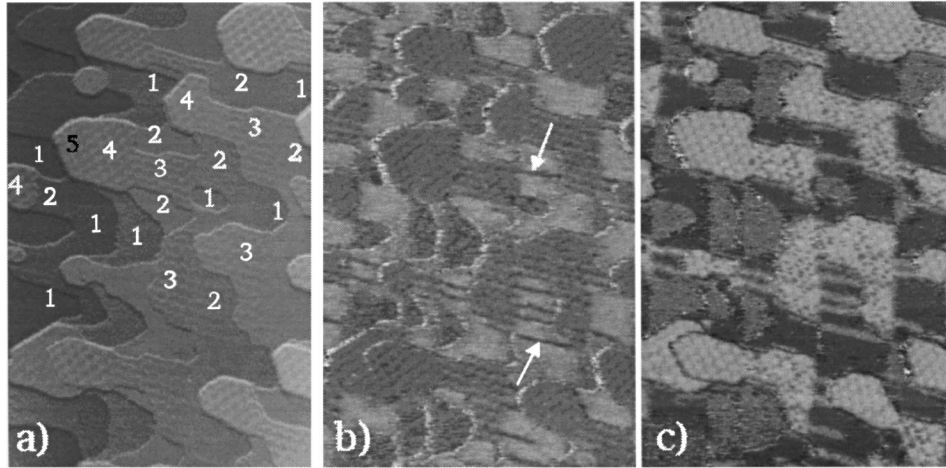


FIG. 3. (a): Topography of a 2-ML Fe film on W(110) after postannealing at a temperature of less than 600 K (scan range: 80 nm \times 120 nm). Fe forms nanometer-scale wedges on the stepped substrate ($1 \text{ ML} \leq \Theta \leq 5 \text{ ML}$). The different regimes of coverage can be distinguished by characteristic dislocation patterns (see text). (b): At $U_{\text{gap}} = 0.4 \text{ V}$, which is close to the position of the empty-state peak described above, the second monolayer has the higher (brighter) differential conductivity dI/dU . The differential conductivity is diminished wherever the Fe film begins to relax, i.e., at dislocation lines in the second monolayer (marked by arrows). (c) At $U_{\text{gap}} = -0.4 \text{ V}$, which is close to the occupied state peak, areas appear bright when the local coverage $\Theta \geq 3 \text{ ML}$. The same is true for the dislocation lines in the second monolayer.

responds nicely with photoemission data from bulk¹⁴ Fe(110) and from Fe/W(110) samples with $\Theta \geq 3 \text{ ML}$.³

We now turn to the question about the nature of the empty-state peak on monolayers and bilayers of Fe on W(110). Since we know that the peak totally vanishes above islands with a height of 4 ML a key for the understanding might be the structural transition in the range between two and four monolayers. Therefore we prepared nanometer-scale wedges of Fe on W(110), which naturally are formed by moderate postannealing. The topography of such a sample is shown in Fig. 3(a). For clarity the local coverage is indicated. In the middle of the image a characteristic wedge is visible which contains a one-monolayer-deep hole in the second monolayer. On any wedge we can observe simultaneously the forthcoming stages of growth of Fe on W(110),¹⁰ i.e., pseudomorphic growth in the first and partially in the second monolayer, nonperiodic and periodic dislocation lines in the second and third monolayer, respectively, and the periodic dislocation network from the fourth monolayer on.

On this sample we measured simultaneously the topography and the spatially resolved differential conductivity dI/dU at different gap voltages. In Figs. 3(b) and 3(c) maps of dI/dU at a gap voltage $U_{\text{gap}} = +0.4 \text{ V}$ and $U_{\text{gap}} = -0.4 \text{ V}$ are presented, which correspond to the empty-state and occupied-state peak positions as seen in Fig. 2(b), respectively. In accordance with the data of Fig. 2(b) the dI/dU signal at $U_{\text{gap}} = +0.4 \text{ V}$ (empty states) is higher above the second monolayer than above the fourth monolayer while the opposite is true at $U_{\text{gap}} = -0.4 \text{ V}$ [Fig. 3(b)]. In the following we want to concentrate on the range of coverage where the transition in the electronic structure occurs, i.e., at $1 \text{ ML} \leq \Theta \leq 3 \text{ ML}$. Obviously the electronic structure changes on a narrow lateral scale. While we measured a high differential conductivity just above E_F for the second monolayer, it is diminished at the dislocation lines (marked by arrows), which exhibit a weak zig-zag structure with a full width of $\approx 15 \text{ \AA}$ and an apparent height of 0.4 \AA in the topographic data. The measured dI/dU signal has the same full width of

$\approx 15 \text{ \AA}$. However, the most important observation is that the behavior of the dI/dU signal at $U_{\text{gap}} = 0.4 \text{ V}$ is almost the same for the dislocation lines in the second monolayer and for locations where $\Theta \geq 4 \text{ ML}$ [Figs. 3(b), 3(c)]. This means that the empty-state peak disappears wherever the Fe film begins to relax. Thus we conclude that the origin of the empty-state peak as seen by STS in the first two monolayers is stress induced due to the relative large lattice mismatch of 9.4%. Our experimental results are in agreement with earlier band-structure calculations for Fe on W(110).⁵ It was shown that the expansion of the lattice constant by 9.4% in the heteroepitaxial Fe overlayer leads to a change of electronic structure of the Fe film which results in an increase of the density of states just above E_F .⁵ According to this band structure calculation the spin polarization at this energy is close to 100%. Thus, similar to the Fe(100) surface,¹⁵ thin Fe films on W(110) might serve as a candidate to perform spin-polarized tunneling experiments.

As mentioned above, the dI/dU signal is not homogeneous on individual islands. Particularly, the amplitude of the empty-state peak shows significant variations. In Fig. 4 we have plotted the cross section of both the topography and the dI/dU signal of an Fe island. Obviously, the apparent height of the island is slightly increased at both edges ($\approx 0.05 \text{ \AA}$) and a decay of the peak height at $U_{\text{gap}} = 0.22 \text{ V}$ close to the island edges is observed. Since the scan speed was extremely low and the feedback was properly adjusted an experimental artifact due to tip-edge interactions can strictly be ruled out. Note that the effects in the topographic and spectroscopic signal were observed while scanning downwards and upwards a step edge. We attribute this decay of the peak height at 0.22 V to a partial relaxation of the Fe close to island edges. Since the number of nearest neighbors for edge atoms is reduced, they do not feel isotropic in-plane forces. One possible explanation for our results is that these atoms are shifted inwards, thus bringing the lattice spacing closer to the Fe bulk value.

In summary, we have observed for the first time, to our knowledge, a stress-induced change of electronic structure in

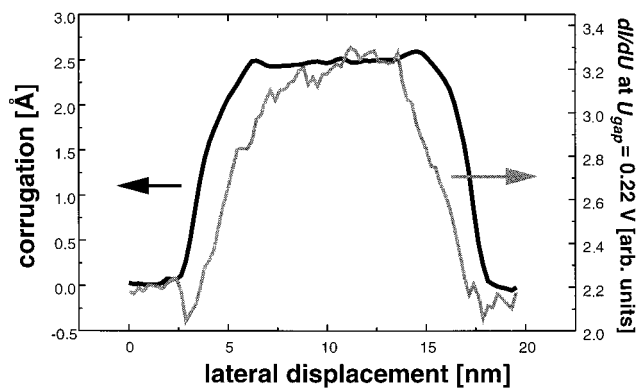


FIG. 4. Topographic (left-hand scale) and corresponding spectroscopic (right-hand scale) line section of the same Fe island. On top of the island close to the edges the apparent corrugation is slightly enhanced and the dI/dU signal is diminished. Since the number of nearest neighbors is reduced at the island edges the outermost atoms are shifted inwards. This causes a lattice spacing which is closer to the Fe bulk value, i.e., a partial relaxation that hinders coalescence of adjacent islands.

heteroepitaxially grown thin films directly in real space by STS. While an empty-state peak in the differential conductivity was found above pseudomorphically grown Fe films on W(110) for $\Theta \leq 2$ ML this peak disappears on a narrow lateral scale wherever the Fe film begins to relax ($\Theta \geq 2$ ML). The resulting influence on the topography and on the differential conductivity has been observed on the same lateral scale of ≈ 15 Å. The results can be explained by a stress-induced change of electronic structure for the pseudomorphic Fe overlayer in agreement with earlier band-structure calculations. Furthermore, our measurements provide the first direct experimental evidence for a partial relaxation at island edges in the first monolayer which hinders island coalescence.

We would like to thank H. J. Elmers and U. Gradmann for helpful discussions. Financial support from the Deutsche Forschungsgemeinschaft (Grant No. Wi 1277/3-1), the Bundesministerium für Forschung und Technologie (Grant No. 13N6500), the European Community (Grant No. BE 7495-93), and the Graduiertenkolleg "Nanostrukturierte Festkörper" is gratefully acknowledged.

- ¹D. P. Pappas, K.-P. Kämper, and H. Hopster, *Phys. Rev. Lett.* **64**, 3179 (1990); R. Allenspach and A. Bischof, *ibid.* **69**, 3385 (1992); J. Thomassen *et al.*, *ibid.* **69**, 3831 (1992); F. Scheuer, R. Allenspach, P. Xhonneux, and E. Courtens, *Phys. Rev. B* **48**, 9890 (1993); D. Li *et al.*, *Phys. Rev. Lett.* **72**, 3112 (1994); F. Ciccacci and S. D. Rossi, *Phys. Rev. B* **51**, 11 538 (1995).
- ²D. Pescia *et al.*, *Phys. Rev. Lett.* **58**, 933 (1987); W. Weber *et al.*, *Nature* **374**, 788 (1995).
- ³R. Kurzawa, K.-P. Kämper, W. Schmitt, and G. Güntherodt, *Solid State Commun.* **60**, 777 (1986).
- ⁴M. Przybylski and U. Gradmann, *Phys. Rev. Lett.* **59**, 1152 (1987).
- ⁵S. C. Hong, A. J. Freeman, and C. L. Fu, *Phys. Rev. B* **38**, 12 156 (1988).

- ⁶W. Weber *et al.*, *Phys. Rev. Lett.* **65**, 2058 (1990).
- ⁷H. J. Elmers and U. Gradmann, *Appl. Phys. A* **51**, 255 (1990).
- ⁸H. J. Elmers *et al.*, *Phys. Rev. Lett.* **73**, 898 (1994).
- ⁹C. H. Back, C. Würsch, D. Kerkmann, and D. Pescia, *Z. Phys. B* **96**, 1 (1994).
- ¹⁰H. Bethge, D. Heuer, Ch. Jensen, K. Reshöft, and U. Köhler, *Surf. Sci.* **331–333**, 878 (1995).
- ¹¹H. J. Elmers *et al.*, *Phys. Rev. Lett.* **75**, 2031 (1995).
- ¹²C. Jensen, K. Reshöft, and U. Köhler, *Appl. Phys. A* **62**, 217 (1996).
- ¹³U. Gradmann and G. Waller, *Surf. Sci.* **116**, 539 (1982).
- ¹⁴P. Heimann and H. Neddermeyer, *Phys. Rev. B* **18**, 3537 (1978).
- ¹⁵J. A. Stroscio, D. T. Pierce, A. Davies, and R. J. Celotta, *Phys. Rev. Lett.* **75**, 2960 (1995).